Title: Cellulose fibrillation and interaction with psyllium seed husk heteroxylan

Author names and affiliations:

Yi Ren[1] yi.ren@nottingham.ac.uk +44(0)1159516012
Bruce R. Linter[2] Bruce.Linter@pepsico.com
Tim J. Foster[1] Tim.Foster@nottingham.ac.uk

[1] Division of Food Sciences, School of Biosciences, University of Nottingham, Sutton Bonington Campus, Loughborough, LE12 5RD, UK
[2] PepsiCo International Ltd, 4 Leycroft Rd, Leicester, LE4 1ET, UK

Highlights:

- Flocculates of fibrillated cellulose is promoted by heating and centrifugation
- Unheated mixtures can be described as binary phase dispersions
- Heated mixtures form interpenetrating composites with psyllium husk heteroxylan
- Psyllium husk heteroxylans weakly associate with (fibrillated) cellulose
- Increased fibrillation leads to a denser or clumped structure of the mixtures

Keywords:

Cellulose fibrillation, Turbiscan, psyllium, heteroxylan, rheological synergism, fluorescence microscopy

Abstract

Fibrillated cellulose (FC) and its mixture with psyllium seed husk powder (PSY) were investigated to broaden the applications of these two materials by a novel combination. Purified cellulose was processed by a colloid mill and relatively stable suspensions were obtained. An FC suspension shows localised concentrations appearing as flocculates, which can be promoted by heating or centrifugation.

The structures of unheated mixtures of FC and PSY appear to be binary phase dispersions while, after heat treatment, FC fibres were incorporated into PSY gels and form composites. Fibrillation on the FC surface does not influence the structure and rheological property of the composite mixtures while fibre disintegration contributes to a denser structure and higher moduli. Fluorescent images show the attachment of PSY heteroxylan aggregates on cellulose and fibrillated cellulose fibres. The interaction is weak and time-dependent because G' during cooling was higher than that during heating, and declined back to the same value as the start of heating during an isothermal test at 20 ºC. PSY was fractionated according to temperature and only F60 (fraction at 60 ºC) clearly associates with the unfibrillated cellulose fibres, possibly via long arabinan sidechains (similar to hairy pectin) or/and backbone (via interaction with helical domains or/and conformational compatibility). The interaction was promoted by fibrillation, potentially trapping PSY heteroxylan aggregates within the cellulose dispersion. With further fibrillation, smaller FC fibres were generated and form interpenetrating particles with whole PSY or PSY fractions. Highly fibrillated cellulose has a higher surface area and smaller fibrils, which significantly increased the interaction resulting in a clumped structure.

1. Introduction

Cellulose exists in the cell wall of plants as a structuring material and it can also be secreted by algae and certain bacteria. There is a growing interest in cellulose treatment and application due to its abundance, biodegradability, and renewability. The cellulose molecule is a β-glucan composed of (1→4) linked D-glucose adopting a flat, 2-fold helical conformation with hydrophobic surfaces and hydrophilic sides of chains where every second glucose unit rotates 180° around the axis of the backbone (Huber, Iborra & Corma, 2006; Wyman et al., 2005). The molecular structure of the individual cellulose chain is stabilised by intramolecular hydrogen bonds between neighbouring glucose. In native cellulose, the glucan molecules associate in parallel into crystalline sections (cellulose I) stabilised by hydrogen bonds and form elementary fibrils (protofibrils) with amorphous sections in between as dislocations (Habibi, Lucia & Rojas, 2010; Pääkkö et al., 2007; Wyman et al., 2005). The elementary fibrils then pack into larger units known as microfibrils with diameters ranging from 2 to 20 nm and amorphous dislocations lead to tilts and twists on the microfibrils. The microfibrils further form macrofibrils with lignin and hemicellulose with complex ultrastructure (Bledzki & Gassan, 1999). In each fibre cell, cellulose fibres are orientated in several layers around a lumen (Bledzki & Gassan, 1999). The cellulose crystalline regions can be in four forms i.e. Iα, Iβ, II and III and cellulose I is the least stable form (Goldberg et al., 2015). Native cellulose is cellulose I, which can be in two forms, cellulose Iα, with a one-chain triclinic unit cell, and Iβ, with a monoclinic two-chain unit cell. Cellulose Iα is secreted by bacteria and algae and cellulose Iβ abundantly exists in the plant cell wall (Nishiyama, Sugiyama, Chanzy & Langan, 2003; Sugiyama, Persson & Chanzy, 1991). Cellulose II can be produced by mercerization and regeneration from cellulose I and cellulose III is generated by mercerizing cellulose I or II in ammonia (Atalla & Vanderhart, 1984; Hebert, 1985; Wada, Chanzy, Nishiyama & Langan, 2004).

Cellulose can be treated either chemically or mechanically to obtain desired functions. Microfibrillated cellulose (MFC) is firstly processed by high pressure and shearing which leads to a physical unwinding of native cellulose fibres and generates highly entangled cellulose fibrils with high surface area, liquid retention, and reactivity (Herrick, Casebier, Hamilton & Sandberg, 1983; Turbak, Snyder & Sandberg, 1983a). MFC is usually in the form of aggregates of cellulose microfibrils (Svagan, Azizi Samir & Berglund, 2007).

Currently, the most widely applied mechanical fibrillation treatments are the application of high-pressure homogeniser and microfluidiser (López-Rubio et al., 2007; Nakagaito & Yano, 2004; Pääkkö et al., 2007; Stenstad, Andresen, Tanem & Stenius, 2008; Zimmermann, Pöhler & Geiger, 2004). Refiners, cryo-crushing, grinders, and extrusion were also used to produce MFC, which sometimes are combined with a high-pressure homogeniser and microfluidiser (Alemdar & Sain, 2008; Heiskanen, Harlin, Backfolk & Laitinen, 2014; Iwamoto, Nakagaito, Yano & Nogi, 2005; Wang & Sain, 2007). The mechanical fibrillation process requires intensive energy input; therefore, pre-treatments are investigated to reduce the energy input. The pre-treatments include purification of cellulose, reducing hydrogen bonds, inducing repulsive force by adding a repulsive charge, decreasing the degree of polymerisation, and/or breaking amorphous regions between individual MFC fibres (Lavoine, Desloges, Dufresne & Bras, 2012; Siró & Plackett, 2010). Most MFC is produced based on cellulose I though MFC of cellulose II has been obtained by a cellulose regeneration process by electrospinning (Li & Xia, 2004; Walther, Timonen, Díez, Laukkanen & Ikkala, 2011). The MFC application can be across different industries such as foods, pharmacy, and cosmetics. In food productions, MFC can be used as a thickener, compounds carriers, and suspension & emulsion stabilisers (Turbak, Snyder & Sandberg, 1982, 1983b).

Cellulose is one of the main components in the plant cell wall and it forms complexes with hemicellulose, pectin and/or lignin to compose the final structure of the cell wall. The composition of non-cellulosic polysaccharides depends on the plant species. Apart from cellulose, the major polysaccharides in type I primary cell wall of most flowering plants are xyloglucan or pectin but that of the primary cell wall (type II) of poaceae are mixed linkage β-D-glucan and heteroxylan substituted with glucuronic acid or arabinose (Carpita & Gibeaut, 1993). The interaction between cellulose and these non-cellulosic materials has been studied to understand their roles in cell wall structuring and functioning. Pectin forms an interpenetrating network with bacterial cellulose when it was added in bacteria culture (Chanliaud & Gidley, 1999; Mikkelsen, Flanagan, Wilson, Bacic & Gidley, 2015). Xyloglucan and mannans bind to bacterial cellulose and form cross-bridges and the galactose content of xyloglucan has a significant effect on the cellulose composites (Mikkelsen et al., 2015; Whitney, Gothard, Mitchell & Gidley, 1999; Whitney et al., 2006). Arabinoxylan and mixed linkage glucan interact unspecifically with the more hydrophobic surface of cellulose via hydrophobic forces (Mikkelsen et al., 2015). The influence of arabinoxylan and mixed

linkage glucan on extensional mechanical properties of plant cell wall cellulose is less significant compared to xyloglucan and pectin (Mikkelsen et al., 2015). Grantham et al. (2017) and Busse-Wicher, Grantham, Lyczakowski, Nikolovski and Dupree (2016) investigated the interaction between acetate and/or glucuronic acid decorated xylan with cellulose in native cell wall material extracted from plant stems. They found that xylan can interact with both the hydrophobic or the hydrophilic surfaces of cellulose depending on the decoration patterns. In addition, mixtures of polysaccharides and cellulose have also been studied. Agoda-Tandjawa, Durand, Gaillard, Garnier and Doublier (2012) investigated the composites of MFC and low-methoxyl pectin which showed different structural and rheological properties. Díaz-Calderón et al. (2018) investigated the mixtures of bacterial cellulose with starch which showed increased viscosity due to water competition and interaction between cellulose and starch. Cellulose and fibrillated cellulose are also widely used to reinforce films and engineering plastic composites (Mohanty, Misra & Hinrichsen, 2000).

In addition, psyllium (*Plantago ovata* Forsk) seed husk is a natural source of dietary fibre, which triggers interests in food and pharmaceutical sciences as a functional ingredient. It has been widely used in gluten free bread as stabilisers. The main compound in the mucilage of the seed husk is β-(1 → 4)-D-heteroxylan substituted on O-3 and/or O-2 positions by arabinose and xylose with complex structures (Edwards, Chaplin, Blackwood & Dettmar, 2003; Fischer et al., 2004; Guo, Cui, Wangb & Young, 2008; Yu et al., 2017). For most substituted xylan, water solubility and extractability increase with higher A/X ratios since arabinose sidechains interfere the interactions between xylan backbones (Andrewartha, Phillips & Stone, 1979; Izydorczyk, Macri & MacGregor, 1998; Mandalari et al., 2005; Zhang, Smith & Li, 2014). However, psyllium husk heteroxylan has low solubility and water extractability although it is heavily substituted (Fischer et al., 2004; Guo et al., 2008; Yu et al., 2017). Psyllium husk polysaccharide shows a gel-like property when hydrated in water though there are differences between fractions extracted by either water or alkaline solutions (Farahnaky, Askari, Majzoobi & Mesbahi, 2010; Guo, Cui, Wang, Goff & Smith, 2009; Haque, Richardson, Morris & Dea, 1993; Ren, Yakubov, Linter, MacNaughtan & Foster, Unpublished results, in preparation; Yu et al., 2017). The influence on the gel properties by the ionic environment, concentration, temperature, and pH has also been investigated (Farahnaky et al., 2010; Guo et al., 2009). Additionally, the property and functionality of

psyllium husk polysaccharides have been modified by the addition of other polysaccharides, phosphorylation or enzymatic treatment (Kale, Yadav & Hanah, 2016; Rao, Warrier, Gaikwad & Shevate, 2016; Yu, DeVay, Lai, Simmons & Neilsen, 2001).

In this study, we investigated cellulose fibrillation using a colloid mill based on the rotor-stator principle, which disrupted particles by high-speed shearing. Another focus was on the mixtures of dispersion/gel of psyllium husk heteroxylan and dispersions of cellulose or fibrillated cellulose (FC). The purpose was to reinforce psyllium husk heteroxylan gel with cellulose or FC to obtain a novel composite with desired rheological property and to broaden its application, e.g. in psyllium-husk containing gluten free bread with the benefit of starch/calorie reduction. The study also deepened the understanding of interactions between psyllium husk heteroxylan and cellulosic ingredients in food products.

2. Materials and methods

2.1. Materials

Pure cellulose powder, Solka floc 900FCC (food grade), was supplied by International Fiber Corporation, US. Psyllium husk powder (Vitacel®, food grade) was kindly donated by the JRS (J. Rettenmaier & Söhne Group, Rosenberg, Germany). Fluorescein isothiocyanate (FITC) was purchased from Acros Organics (New Jersey, US). Methyl blue was purchased from Sigma–Aldrich (UK). FITC and Methyl blue were of analytical grade.

2.2. Cellulose fibrillation and influences of processing time

The cellulose was fibrillated using a colloid mill (Winkworth, Basingstoke, UK) at a rate of 2 min L^{-1}, 4 min L^{-1}, 10 min L^{-1}, 20 min L^{-1}, 40 min L^{-1}, or 60 min L^{-1} labelled as FC2, FC4, FC10, FC 20, FC40, or FC60. The unfibrillated sample was labelled as FC0. The colloid mill was adjusted to the smallest gap and 5 g of cellulose were dispersed in 500 mL of RO water as one batch.

The freshly fibrillated samples were tested by Turbiscan Lab (Formulation, L' Union, France) at 25 °C and imaged by light microscopy (Evos FL, Waltham, US) immediately after being processed. The stability of freshly fibrillated cellulose was calculated as the Turbiscan stability index (TSI) by Turbisoft 2.2 using equation (1). $Scan_i(h)$ minus $scan_{i-1}(h)$ is the difference in the averaged backscattering between two measurements. H is the sample height.

$$TSI = \sum_i \frac{\sum_h |scan_i(h) - scan_{i-1}(h)|}{H} \quad (1)$$

The freshly prepared FC were also stored at 20 °C and 80 °C and tested by Turbiscan. The samples were gently shaken by hand to redisperse the suspensions before each scan so the flocculation of fibrils can be solely tested excluding sedimentation.

Freshly prepared FC60 was also centrifuged at 4000 g, 4 °C, for 15 min. The sediment was collected and recovered back to the original concentration, i.e. approximately 0.77% (w/w). The recovered suspension was rehomogenised using an Ultra-Turrax homogeniser (T25, Ika®-Werke, Germany). The freshly prepared, recovered and rehomogenised FC60 were scanned by Turbiscan.

To prepare stock suspensions of FC, the freshly processed FCs were centrifuged at 4000 g, 4 °C, for 15 min. The residues in supernatants, which were discarded, were checked to be less than 0.01% by drying at 105 °C. The concentration of sediment, which was collected, was verified by drying at 105 °C for each batch. The stock FC suspensions were kept at 4 °C. The stock suspensions were diluted to the required concentration and mixed via vortex for 2 min for further sample preparations and tests.

2.3. Time-domain NMR measurement

Proton relaxation measurements were performed with an R4 Benchtop NMR System (Advanced Magnetic Resonance Ltd, Abingdon, U.K.) equipped with a thermal controller (Advanced Magnetic Resonance Ltd). The transverse relaxation curves were obtained by the Carr-Purcell-Meiboom-Gill (CPMG) sequences (Meiboom & Gill, 1958), beginning with a 90° pulse followed by 32768 180°-pulses with 0.256 ms (TAU) between every two pulses. The 90° pulse for all sequences was approximately 2.6 µs and the signals were recorded 5 µs (dead time) after the pulse. Each CPMG sequence was repeated 64 times on each sample to obtain the average values. The samples were allowed to relax for 10 seconds between every two scans.

2.4. FC-PSY mixture preparation

Psyllium seed husk powder (PSY) was dispersed in RO water at a concentration of 1.64% or 0.82%. The concentration was decided during the formulation optimisation of gluten free

bread. Stock suspensions of FC10 and FC60 were diluted to 1.64% or 0.82% (w/w) by vortexing for 2 minutes and 1.64% and 0.82% FC0 were prepared by suspending pure Solka floc 900FC cellulose in RO water. The PSY suspension (1.64%) was then mixed with 1.64% FC suspensions immediately at a 1:1 ratio by weight. The mixtures were stirred slowly (less than 100 rpm) at room temperature for 1 hour. The heat treatment was performed by incubating samples in a boiling water bath with slow stirring (less than 100 rpm) for 20 minutes followed by cooling at room temperature for 1 hour.

2.5. Rheological properties

Dynamic oscillatory shear tests were performed using an MRC 301 rheometer (Anton Paar, Austria), with parallel plate geometry including a sandblasted upper plate (PP50-SN11649, Anton Paar). The measuring gap was 1 mm. The temperature was controlled by a Peltier system with the assistant of a water bath (R1, Grant, Shepreth). Unheated samples and heated FC60 suspensions were loaded at 20 °C and held for 500 seconds before tests. The PSY containing samples which underwent heat treatment were loaded at 20°C then the temperature was increased to 60 °C and maintained for 5 min to melt the gels and release the energy stored due to normal stress induced by compression. Waiting time was also 500 seconds at 20 °C before tests. Frequency sweep tests were performed in the range of 100 to 0.1 rad s^{-1} with the angular frequency decreasing logarithmically. Temperature sweep tests were performed on unheated PSY-containing samples where the temperature increased from 20 °C to 98 °C, held for 10 minutes, and cooled back to 20 °C. The temperature ramps were conducted at 1 °C min^{-1}. Two cycles of heating and cooling were applied with 2 hours holding time at 20 °C in between. The strain (0.2%) used was in the LVE region decided by amplitude sweep tests and the angular frequency used in temperature sweep tests was 10 rad s^{-1}. The edge of samples was trimmed and covered by low viscosity mineral oil (Sigma, USA) to prevent drying of samples. All measurements were performed at least twice and representative curves are presented.

An index R was calculated by equation (2) describing the rheological synergism behaviour of FC-PSY mixtures (Agoda-Tandjawa et al., 2012). G' at angular frequencies of 0.1, 1, and 10 rad s^{-1} were adopted to calculate R individually.

$$R = \frac{G'_{FC+PSY} - (G'_{FC} + G'_{PSY})}{G'_{FC} + G'_{PSY}} \quad (2)$$

2.6. Sample labelling and fluorescence microscopy

2.6.1. Covalent labelling

PSY was stained by FITC covalently either on the surface of the powder particles ($PSY_{toluene}$) or on the molecular levels (PSY_{DMSO}). Additionally, PSY was fractionated by temperature and the procedure was described in the previous paper (Ren et al., Unpublished results). The obtained fractions (F20, F40, F60 and F80) were also labelled by FITC covalently ($F20_{DMSO}$, $F40_{DMSO}$, $F60_{DMSO}$, and $F80_{DMSO}$). More specifically, 0.05g of FITC was dissolved in 50 ml of toluene for surface labelling or in DMSO for molecular level labelling. Then the whole PSY or PSY fractions (0.5g) were dispersed followed by adding 0.1 ml of pyridine and 0.047 ml of dibutyltin dilaurate. The reaction was executed with stirring at 100 ℃ in a closed system purged with nitrogen for the first 2 hours. After reacting for 24 hours, 200 ml of ethanol was poured into the DMSO mixture followed by incubating at 4℃ overnight. The precipitate was then washed by ethanol by multiple centrifugation steps at 2000 g, 4℃, for 10 minutes. As for the toluene reacting mixture, the stained psyllium husk powder was directly washed by ethanol. The labelled samples were vacuum dried at 35℃.

2.6.2. Non-covalent labelling and image acquisition

A small amount of saturated methyl blue was added into 1.64% FC0, FC10, or F60 suspensions and left for 30 minutes. The unheated PSY-FC mixtures were prepared with $PSY_{toluene}$ via the procedure described in section 2.4 that 1.64% $PSY_{toluene}$ was mixed with 1.64% stained FCs by 1:1 ratio and incubated for 1 hour at room temperature with slow stirring. PSY and PSY fractions stained with FITC in DMSO were used to prepare heated samples. PSY_{DMSO}, $F20_{DMSO}$, $F40_{DMSO}$, $F60_{DMSO}$, and $F80_{DMSO}$ were dispersed in RO water by drastic overnight stirring (1000 rpm roughly) at room temperature. They were then mixed with methyl blue stained FC suspensions with the same concentrations respectively by a 1:1 (w:w) ratio and incubated at room temperature with slow stirring for 1 hour. Heat treatment was described in section 2.4 that the mixtures were heated in a boiling water bath for 20 minutes and cold at room temperature for 1 hour. The samples were scanned by fluorescence microscopy (Evos FL, Waltham, US) equipped with a DAPI (357/44 - 447/60 nm) light cube

and a GFP (470/22 - 525/50 nm) light cube. At least three fluorescence microscopic images or light microscopy images were taken for each sample at each magnification of x 2 or x 10/20.

3. Results and discussion

3.1. Cellulose fibrillation and process time

Pure cellulose powder was fibrillated using a colloid mill and the stabilities of freshly processed suspensions were evaluated by Turbiscan. The calculated TSI is shown in Figure 1a. A higher value of TSI indicates lower stability and faster sedimentation. FC processed for a longer time was more stable as TSI was lower and increased more slowly during storage. They occupied more volume after 4-day storage, as shown in Figure 1b. The less processed FCs settled faster and reached relative stability earlier than FCs processed for longer times, as shown in the insert of Figure 1a, which magnifies the first 1000 s. The microstructures of the FCs are shown in Figure 2. The untreated cellulose (FC0) had long fibres with a relatively smooth surface with kinks and bends. After processing even for a short time, fibrillation became evident (Figure 2 column b). The fibrillation also caused significant effects on the kinks and ends which were weaker points on the fibres (Figure 2 column c). With the processing time increasing up to 10 minutes per litre (FC10), the fibrillation treatment mainly affected the surface of cellulose fibres. With the further processing, most cellulose fibres lost their structure and were fully or partially processed into smaller fibrils (FC40c and FC60c), where the FC suspension showed uneven and localised concentrations appearing as aggregates or flocculates (column a). FC40 and FC60 did not show a significant difference while there were some intact virgin cellulose fibres. The remaining large fibres and unfibrillated fibres were also observed by Herrick et al. (1983) and Andresen, Johansson, Tanem and Stenius (2006). Hence, cellulose was successfully fibrillated to a lower level by colloid mill but further fibrillation requires higher energy input by other equipment such as high-pressure homogeniser.

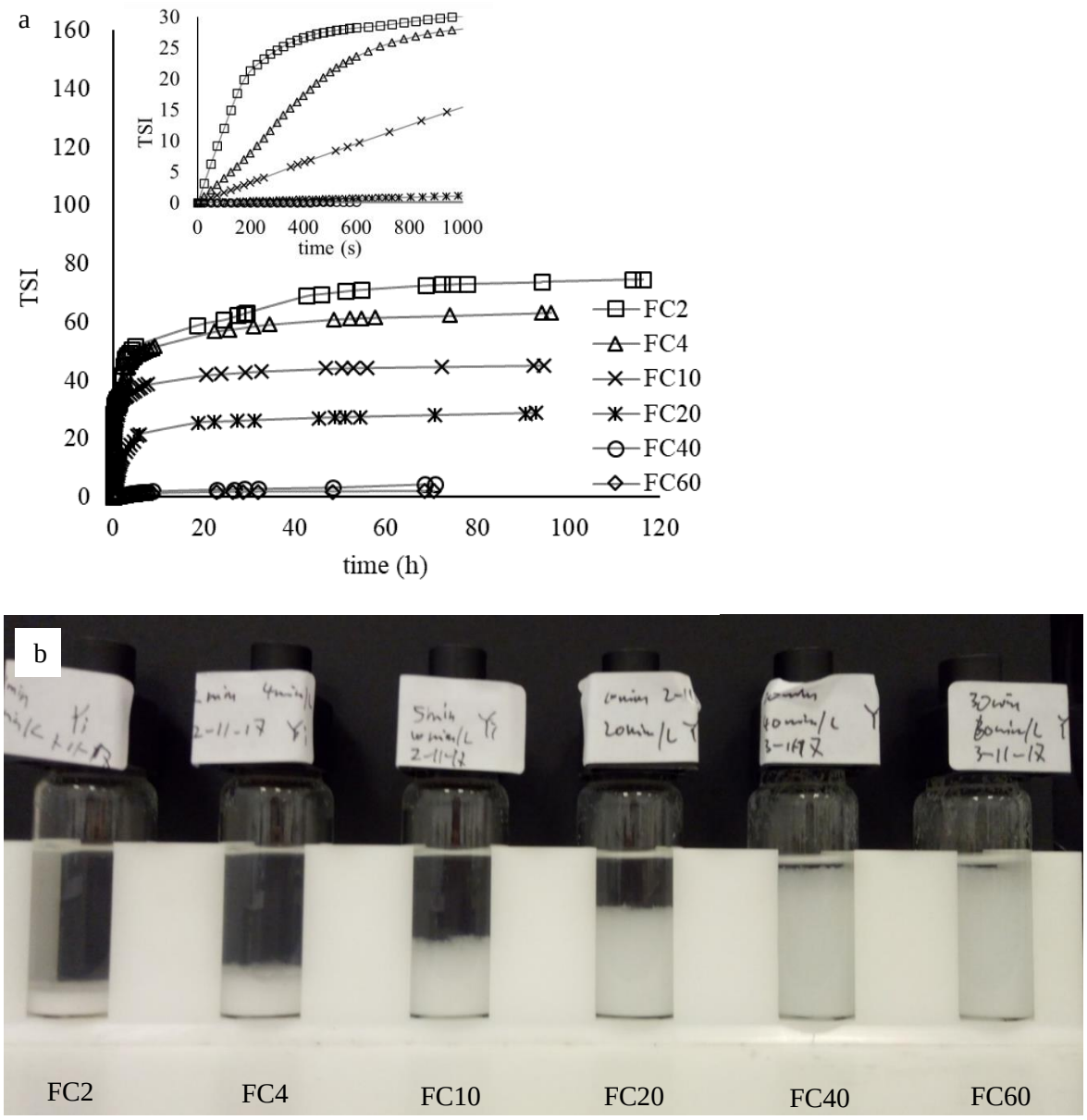

Figure 1. TSI of FC processed for different time (a) and the samples after 4-day storage (b). The insert shows the details of the first 1000s of Figure 1a.

To evaluate the effects of processing on water mobility, FC0, FC10, and FC60 suspensions were evaluated by time domain ^{1}H NMR and the T2 spectra are shown in Figure 3. The T_2 spectrum of FC0 showed three peaks at 2477, 534 and 132 ms. The peak at 2477 ms was due to the bulk water, whereas the other two peaks were assigned to water molecules in the system with different constraint levels. Water in hydrated cellulose includes non-interacting water, interacting water, and proton exchangeable water (Ibbett, Wortmann, Varga & Schuster, 2014). The bound water has very short relaxation time, less than 10 ms, and water trapped by capillary forces in the lumen contributed to a peak at 110 ms (Felby, Thygesen,

Kristensen, Jorgensen & Elder, 2008). However, in Figure 3, the bound water was not detected and water held by capillary forces only is seen as a small peak at 132 ms due to low concentration applied. The T_2 peak at 534 ms was assigned to water weakly interacting with cellulose surface. T_2 spectra of FC10 showed two peaks. The broad peak ranged from 600 to 3000 ms indicating that more water molecules were interacting with cellulose surface as fibrillation significantly increased the total surface and the exposure of hydroxyl groups. With an increase in processing time, FC60 showed one sharp peak at 614 ms which indicates that a large number of water molecules were interacting with cellulose. The lower T2 value indicates reduced water mobility and the narrow peak width suggests that a more uniform suspension was obtained.

Drying MFC leads to the formation of bundles and agglomerates due to the decreased distances, increased contacts and hydrogen bond formation between fibres (Quiévy et al., 2010). In conventional oven drying, there are two main factors, i.e. high temperature and reduced distances between fibres. These two factors were isolated as heat treatment in a sealed system and centrifugation respectively. To evaluate the effects of heat treatment on the flocculation of the FC dispersions, FC0, FC10 and FC60 were stored at 20 °C or 80 °C for 12 days and evaluated by Turbiscan. In Turbiscan analysis, the sedimentation was eliminated by gently redispersing samples before each scan. The changes of backscattering (ΔBS) were calculated taking the first scan as reference shown as a straight line with a value of zero in **Error! Reference source not found.**. It can be seen that the samples stored at 20 °C did not show significant ΔBS while ΔBS increased when they were stored at 80 °C and the increase was already significant during the second scan. The backscattering (BS) increases with the increase of particle size for small Rayleigh – Debye scatterers with the diameter smaller than approximately 0.3 μm (d*), while it decreases with particle size increase when the diameter is larger (Mengual, Meunier, Cayré, Puech & Snabre, 1999). It suggests that high temperature leads to flocculation or aggregation of FC fibres in a smaller size scale (< d*). The enhancement of fibre flocculation is due to the altered thermodynamic state of the dispersion.

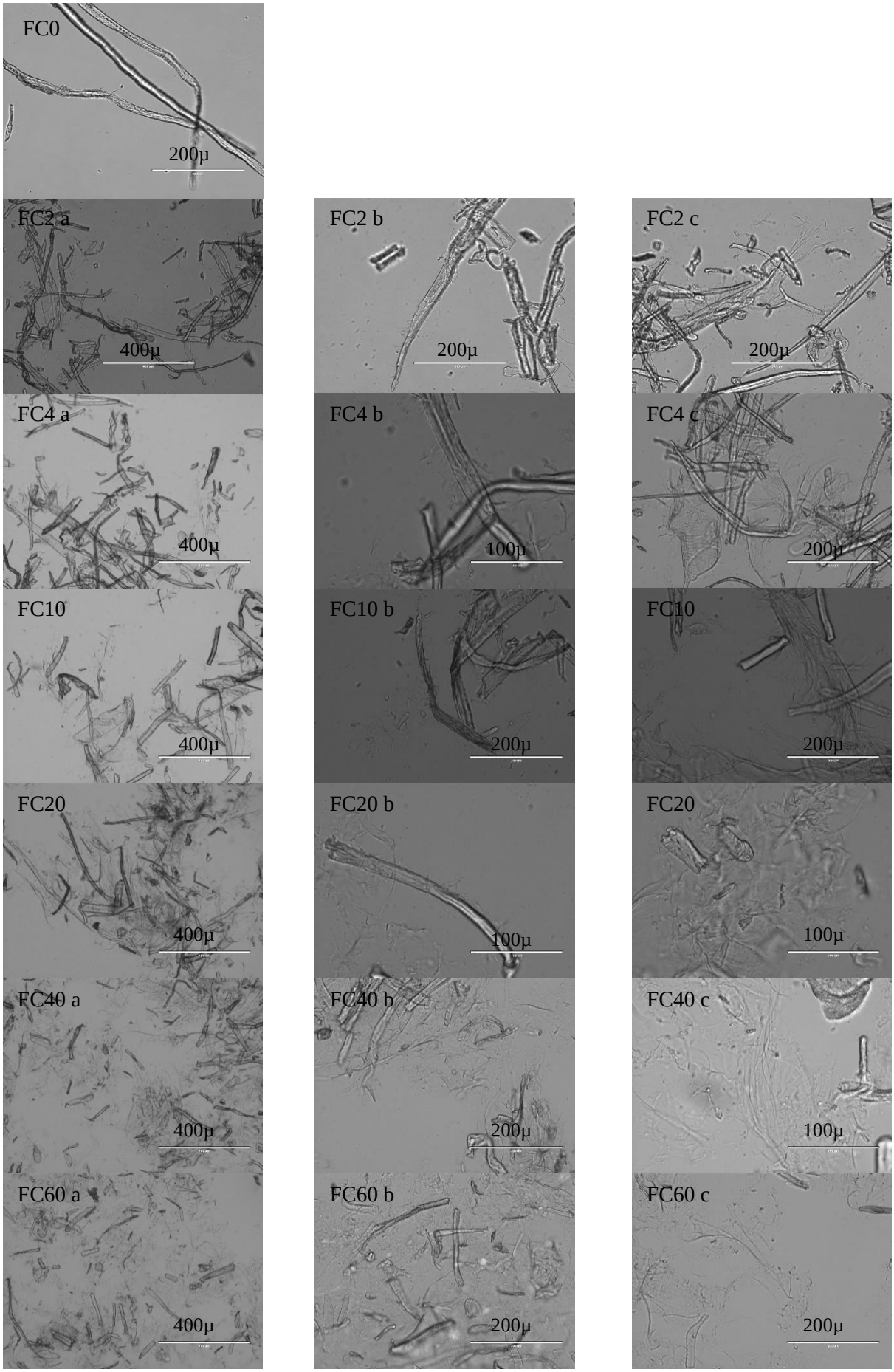
FC0
200µ
FC2 a
400µ
FC2 b
200µ
FC2 c
200µ
FC4 a
400µ
FC4 b
100µ
FC4 c
200µ
FC10
400µ
FC10 b
200µ
FC10
200µ
FC20
400µ
FC20 b
100µ
FC20
100µ
FC40 a
400µ
FC40 b
200µ
FC40 c
100µ
FC60 a
400µ
FC60 b
200µ
FC60 c
200µ

275

Figure 2. Optical micrographs of FC0 (untreated cellulose), FC2, FC4, FC10, FC20, FC40, and FC60, focusing on the overall distribution (column a), fibrillated from the main cellulose fibres (column b), and fibrillated from the edges of main cellulose fibres (column c). Representative images are shown from image acquisitions in at least triplicate.

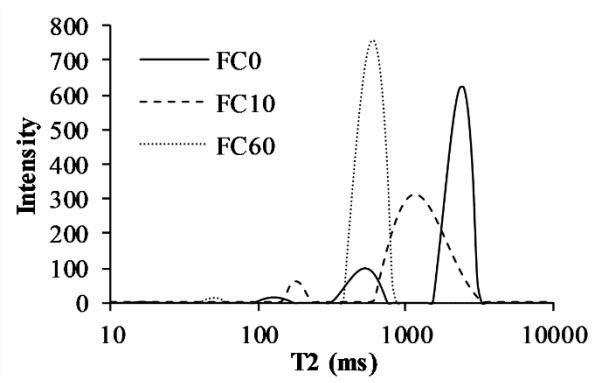

Figure 3. Distribution proton transverse relaxation times (T2) of 1.64% FC0, FC10, and FC60 measured with CPMG sequence.

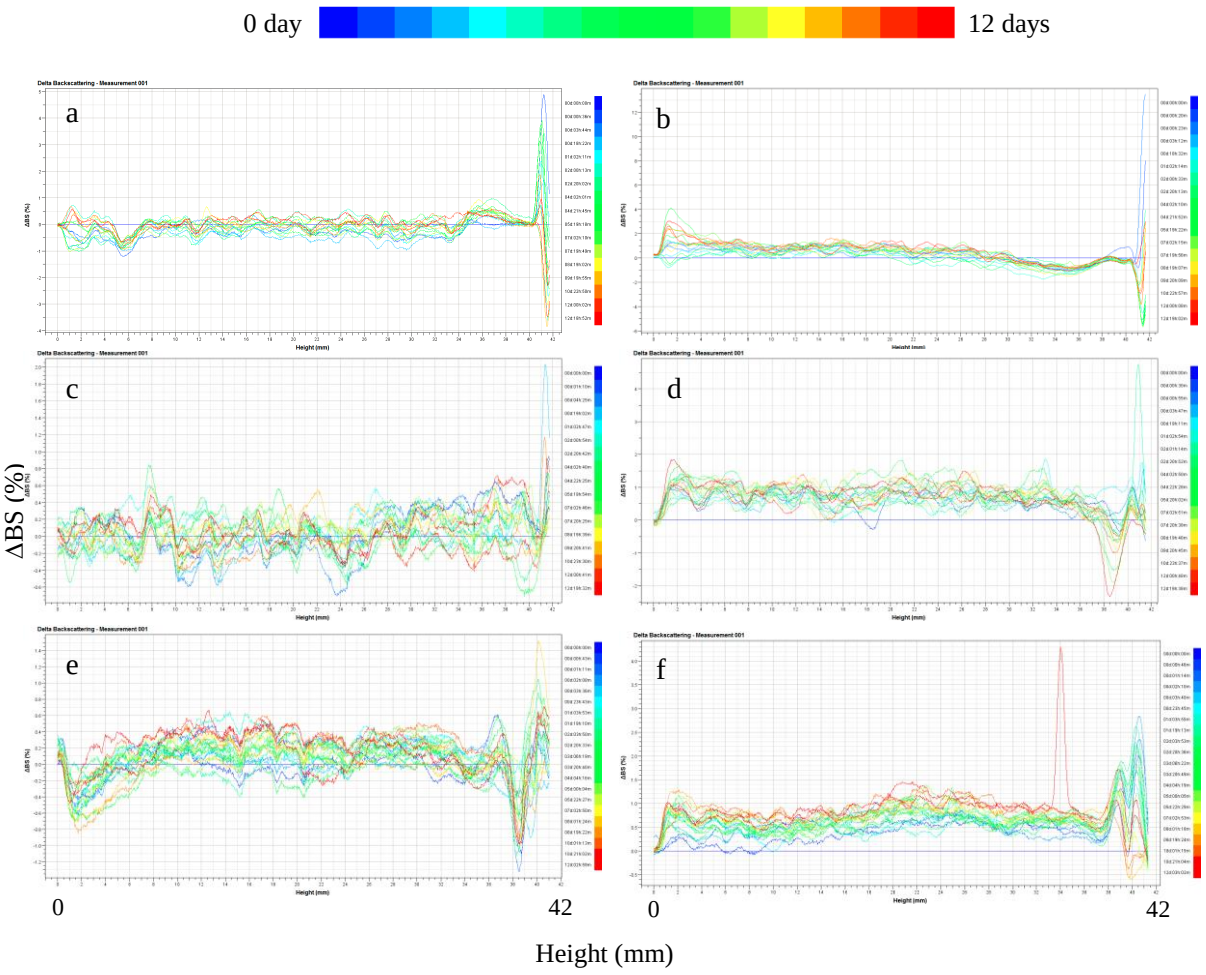

Figure 4. Delta backscattering of FC0 (a), FC10 (c), and FC60 (e) stored at 20 °C and FC0 (b), FC10 (d), and FC60 (f) stored at 80 °C.

In order to evaluate the influences of reduced distances between fibres on the flocculation of FC dispersions, freshly prepare FC60 was centrifuged and recovered in RO water to its original concentration (0.77%). Part of the recovered FC60 was rehomogenised using an Ultra-turrax. The BS of freshly prepared, recovered, and rehomogenised FC60 are shown in Figure 5. BS of recovered FC60 was lower than a freshly prepared suspension, which indicates a promoted flocculation or aggregation at a larger scale (> d*) which is also evidenced by a decrease in shear viscosity (data not shown). It might because of the significant reduction in distances and more extensive formation of hydrogen bonds between FC fibres. Flocculation induced by centrifugation led to BS decreases (< d*) while heat-induced flocculation showed BS increase (> d*), therefore, it can be deduced that the centrifugation (distance)-induced flocculates are larger than heat-induced flocculates. The flocculation can be fully or partially reduced back to the freshly prepared sample by high-speed shearing as BS of rehomogenised FC60 was close to the freshly prepared one. These were also evidenced by a recovery of shear viscosities (data not shown).

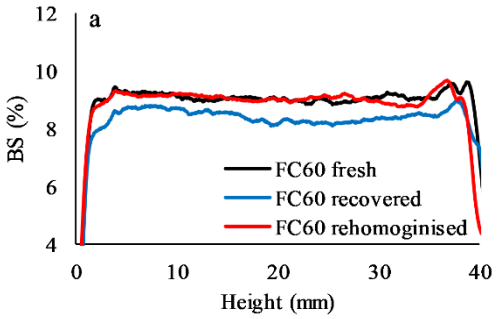

Figure 5. Backscattering of freshly prepared, recovered, and rehomoginised FC60 measured Turbiscan at 20 °C.

3.2. FC and psyllium heteroxylan interaction

3.2.1. Interactions between psyllium and FCs

The mechanical spectra and temperature dependence of rheological parameters of heated and unheated PSY (1.64% or 0.82%) and FC-PSY mixtures (at a total concentration of 1.64%) are shown in Figure 6a and b. The storage modulus of all samples was higher than loss modulus (G' > G'') over the frequency range applied, suggesting gel-like behaviour. Before heat treatment, 0.82% FC and PSY mixtures showed higher moduli and lower frequency dependence than 0.82% PSY, of which the slope of logG' versus logω was 0.32, and these differences became more pronounced when fibrillation processing time increased (FC60-

PSY > FC10-PSY > FC0-PSY with the slopes of logG' versus logω of 0.13, 0.20 and 0.28 respectively) (Figure 6a). FC60-PSY showed even higher moduli than 1.64% PSY. The slope of logη* versus logω became steeper, ranging from -0.62, -0.69, -0.78, -0.87, to -0.93 in the sequence of 0.82% PSY, FC0-PSY, FC10-PSY, FC60-PSY, and 1.64% PSY. Therefore, FC processed for a longer time is more dominant in the overall viscoelastic property of an unheated FC and PSY mixture. After heat treatment, there was no significant difference between FC0-PSY and FC10-PSY while FC60-PSY showed higher moduli (Figure 6b). All spectra showed a similar frequency dependence with a similar logG' versus logω slope of 0.12, though that of 1.64% PSY (0.15) was higher. They also showed a similar logη* versus logω slope of -0.88. A similar value of -0.8 was reported by Whitney et al. (1999) which was analogous across cellulose based cell wall materials from tomato and onion obtained by different extraction methods. Comparing unheated and heated FC-PSY mixtures (Figure 6a and b), when the FC was processed for a longer time, the difference between unheated and corresponding heated mixtures was reduced. Considering the heat treatment has less effect on FC than PSY, this further evidences that FC processed for a longer time becomes more influential in determining the rheological behaviour of the mixtures.

The temperature dependence of G' of 0.82% PSY, 1.64% PSY, and 0.82% FC and PSY mixtures are shown in Figure 6c and d. As reported in the previous study (Ren et al., Unpublished results), PSY suspensions melt during heating and show a stronger gel-like property after first cooling (Figure 6c). This behaviour was also observed when PSY was mixed with FCs (Figure 6c). At the end of cooling of the first cycle, stronger gel-like properties were shown as much higher G' than the value before first heating. Additionally, the overall G' of the mixtures increased with the increase of FC processing time. Figure 6d shows the G' profile during the second heating-cooling cycle. Similarly, the overall G' increased when FC was processed for a longer time. It is noticed that PSY alone showed thermo-reversible behaviour, with G' traces overlapping during heating and cooling. However, PSY-FC mixtures tend to show that G' during cooling was higher than that during heating, which is different from the thermal hysteresis behaviour of other polysaccharides or polysaccharide mixtures where, usually, G' during heating is higher than G' during cooling because of delayed recovery of molecular association or structuring during cooling. Furthermore, G' declined gradually during isothermal tests at 20 ℃ after both first and second heating-cooling cycles, shown as a vertical line at 20 °C on the graphs. After the

second heating-cooling cycle, G’ decreased back to the same value as that before the start of second heating cycles. It suggests time-dependent reversible rheological behaviour of the mixtures. Therefore, it can be speculated that PSY heteroxylan interacts with FCs in the mixtures. It is likely that the interaction is weak and time-dependent.

3.2.2. FC60 and PSY mixtures and rheological synergism

In order to further understand the interactions between FC and PSY and the rheological synergistic behaviour, the mixture of FC60 and PSY were further investigated as FC60 at low concentration (0.82 or 1.64%) is stable for rheological measurements. The mechanical spectra of 0.82% FC60, PSY and their admixture at an individual concentration of 0.82% are shown in Figure 7a and b with and without heat treatment, respectively. The unheated 0.82% PSY (Figure 7a) presented very close G’ and G’’ though G’>G’’. However, 0.82% FC60 displayed a much stronger gel-like property as G’ was much higher than G’’ and less dependent on the angular frequency with a logG’ versus logω slope of 0.06. G’ of the FC60-PSY mixture is slightly more dependent on angular frequency (logG’ versus logω: 0.13) than that of 0.82% FC60 alone, although it has higher moduli than either 0.82% FC60 or PSY. After heat treatment (Figure 7b), these three samples are similar in terms of the overall profiles of oscillatory tests parameters especially the G’ dependence on angular frequency (logG’ versus logω: 0.12 for 0.82% FC60-PSY and PSY but 0.06 for 0.82% FC60), even though the mixture displayed higher moduli. The slope of logη* versus logω was -0.925 for 0.82% FC60, which was similar to that of 1.64% FC60 regardless of heat treatment. Nevertheless, slopes were -0.88 for 0.82% PSY and 0.82% FC60-PSY, which were similar to the mixtures with FC0 and FC10 (Figure 6b). It is obvious that the heated PSY is dominant in determining the logη* versus logω slope of the mixtures with a characteristic value of -0.88.

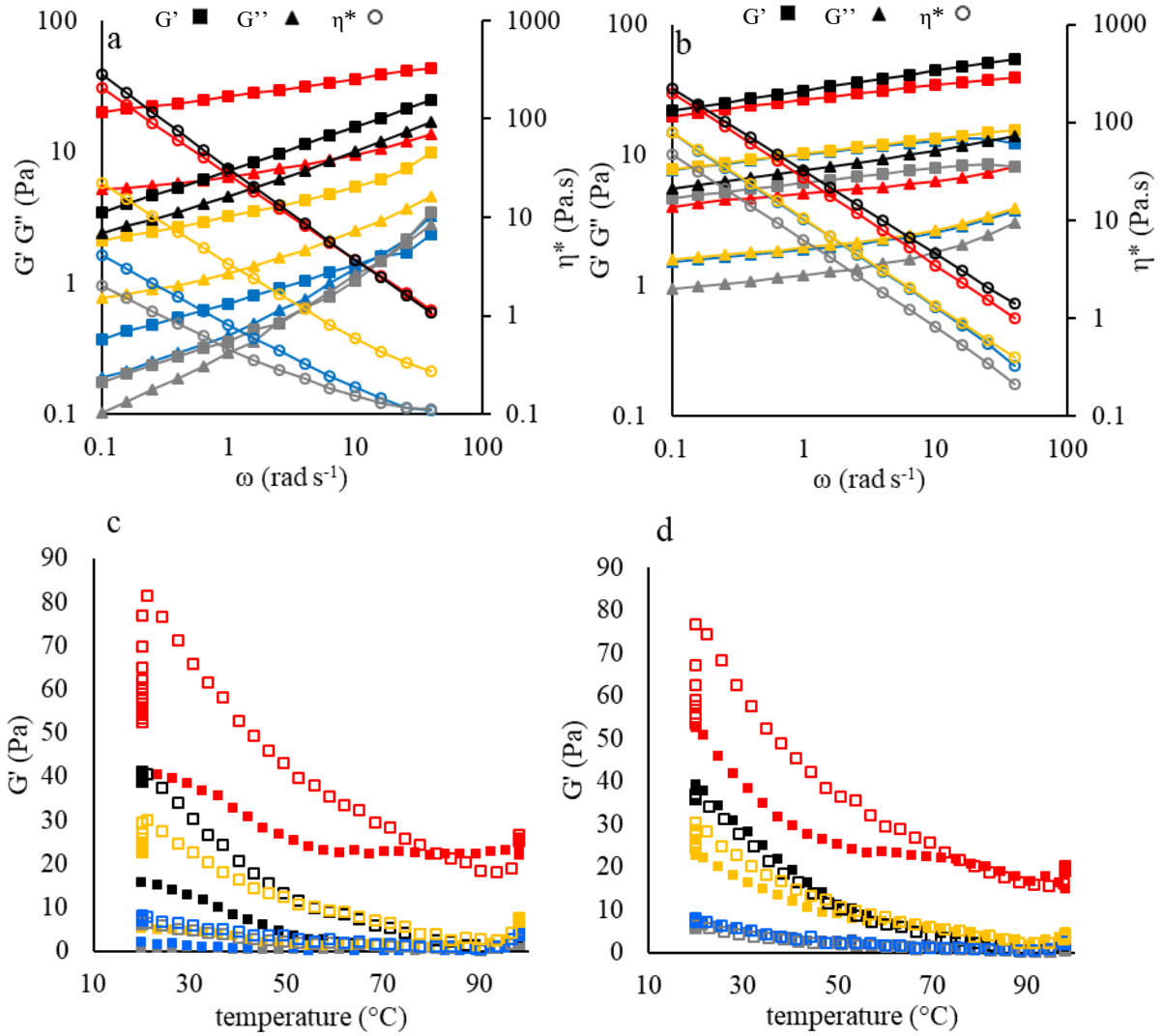

Figure 6. Mechanical spectra of 0.82% PSY (grey), 1.64% PSY (black), and mixtures (0.82%, 1:1 mixing ratio) of PSY and FCs: 0.82% FC0-PSY (blue), FC10-PSY (yellow), FC60-PSY (red), before (a) and after (b) heat treatment, G', square; G'', triangle; η*, circle. Temperature dependence of G' during first heating (solid square) and cooling (open square) cycle (c) and second heating (solid square) and cooling (open square) cycle (d). Strains used were in the LVE region and angular frequency was 10 rad s^{-1} in temperature sweep tests. Plots are shown as representative curves from experiments run in at least duplicate.

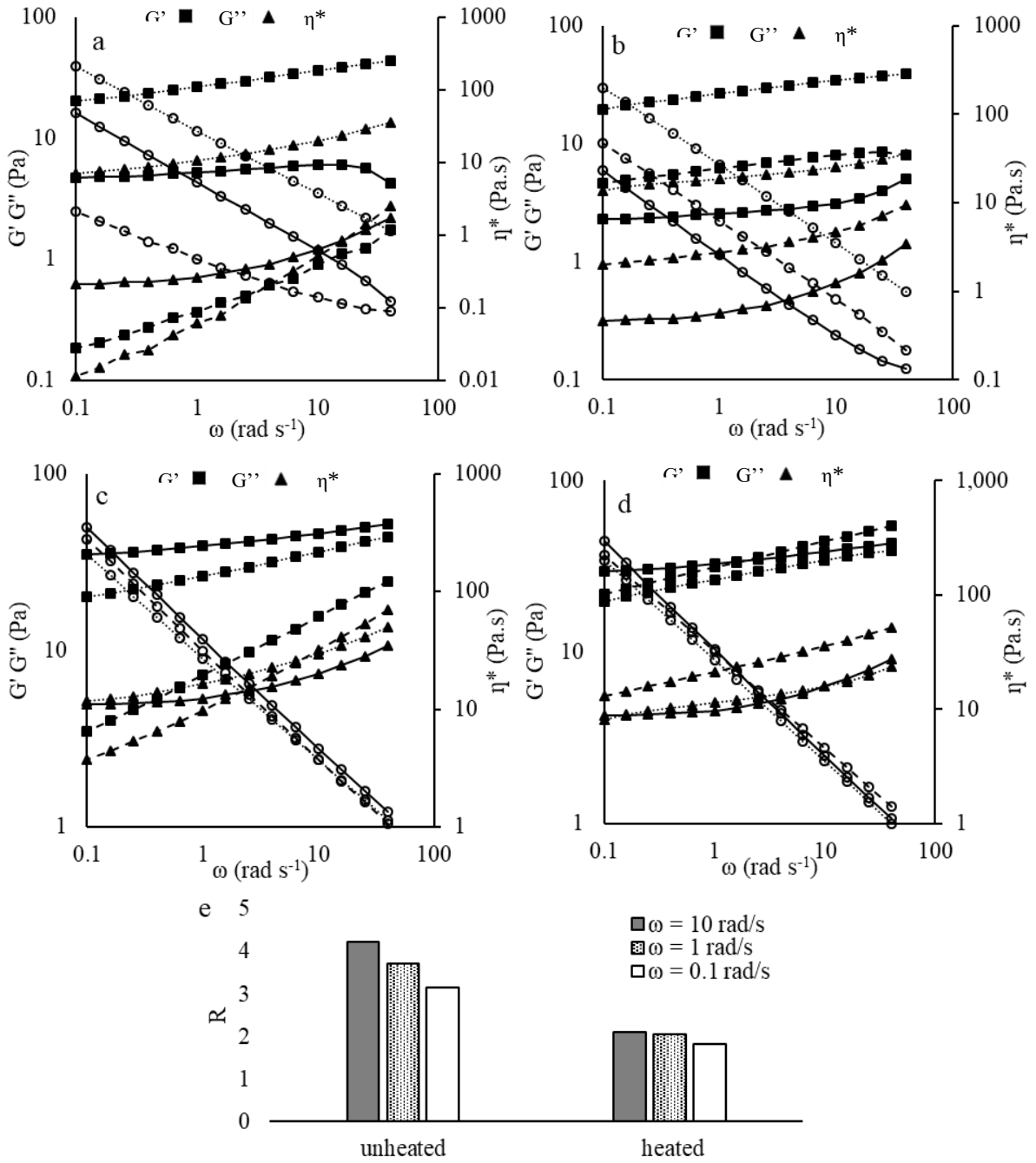

Figure 7. Mechanical spectra of 0.82% FC60 (solid line), 0.82% PSY (thin dashed line), and 0.82% FC60-PSY (dense dashed line), before (a) and after (b) heat treatment. Mechanical spectra of 1.64% FC60 (solid line), 1.64% PSY (thin dashed line), and 0.82% FC60-PSY (dense dashed line), before (c) and after (d) heat treatment. e: R value of unheated and heated 0.82% FC60-PSY calculated by G' values at 0.1, 1, and 10 rad s^{-1}.

The rheological parameters of dynamic oscillatory measurements of 1.64% FC60, 0.82% FC60-PSY, and 1.64% PSY are plotted in Figure 7c and d. The 50% replacement of unheated PSY by FC60 suspensions significantly increased the moduli and gel-like behaviour (less

dependent G' on ω, logG' versus logω: 0.13 for 0.82% FC60-PSY and 0.33 for 1.64% PSY) although it was still lower than 1.64% FC60 which showed more pronounced solid-like property shown as the more significant difference between G' and G''. After being heated, G' of FC60, PSY and their admixture at the same total concentration of 1.64% were less diverse in values, although G'' of PSY was apparently higher than the other two which indicates that more energy was dissipated during small amplitude shear deformation, while the replacement by FC60 significantly deduced the energy loss. In addition, the reduced ω dependence of G' by FC60 addition (0.82% FC60-PSY) was also observed which laid between 1.64% FC60 and PSY (logG' versus logω: 0.06 for FC60, 0.11 for FC60-PSY and 0.15 for PSY). In conclusion, FC60 is more gel-like than PSY as it showed higher moduli and less dependent G' and it is dominant in the mixtures in terms of these two factors, while PSY governs the resistance of mixtures in the viscoelastic flow represented as complex viscosity.

In terms of rheological synergism, an index R was calculated and plotted in Figure 7e. The index R was calculated by equation (2) from the experimental data G' at the angular frequency of 0.1, 1 or 10 rad s^{-1} of either heated or unheated mixtures. The positive R suggested rheological synergism and the addition of FC60 enhances the gel-like property of PSY. However, it is reduced by heat treatment shown as lower synergistic value R.

Mixtures can be 'compatible' and not drive to distract phase that is thermodynamically incompatible. However, if they are, the evidence shows that competition for hydration of mixed dispersions may affect expected rheological properties. It has been observed in the mixtures of xanthan and starch, cellulose ethers and starch, and bacterial cellulose and starch (Díaz-Calderón et al., 2018; Foster et al., 2007; Sullo, 2012). The final endpoint can also be molecular interactions. In the case of mixed dispersions, this would be a result of particulate interaction at the particle surface. The following experiments investigated whether these different phenomena are at play.

3.2.3. Fluorescence microscopy

The microstructure of the PSY and FC mixtures were explored using fluorescence microscopy images. Figure 8 shows the fluorescent images of unheated and heated mixtures of PSY and FCs with a total concentration of 1.64%, where PSY was covalently labelled by FITC shown in green in the images. In unheated mixtures with FC0 and FC10, as circled in

415 red, unheated PSY presented as hydrated and swollen gel particles with an insoluble core
416 (visible under polarised light, image not shown) which was also detailed in Ren et al.
417 (Unpublished results). FCs are not specified in colour but they were visible because of light
418 diffraction. As shown in the images, the phase surrounding hydrated PSY particles were
419 concentrated in FC0 or FC10 fibres. In the previous study (Ren et al., Unpublished results),
420 the freshly prepared PSY suspensions can be described as concentrated suspension of gel
421 particles and its rheological properties can be ascribed to physical forces between these soft
422 particles. In the case of FC0-PSY and FC10-PSY, they can be considered as mixtures
423 consisting of two phases where one phase is hydrated PSY particles distributed in the other
424 one which is concentrated in FC fibres. Therefore, the overall rheological property of the
425 mixture is highly dependent on the strength of FC fibres and the volume taken by them. FC60
426 was highly fibrillated and the FC fibres were not easily distinguished from PSY, therefore the
427 transmitted light image of FC60-PSY was overlaid with the fluorescent images. Although
428 FC60-PSY also consisted of hydrated PSY particles and the surrounding phase of FC60 and
429 PSY gels, the structure was distinctly denser than FC0-PSY and FC10-PSY with higher
430 moduli (Figure 6b). This can be attributed to the fact that FC60 fibres occupied a larger
431 volume than the unfibrillated and less fibrillated cellulose and they competed for water and
432 space with PSY. The water and space competition originating from thermodynamic
433 incompatibility between PSY and FC60 leads to the rheological synergism in the mixture
434 (Figure 7e).

435 In heated samples (Figure 8b), the intact swollen PSY parties were not observed. Instead, FC
436 fibres were incorporated into PSY gels and formed composites, where FC0-PSY b and FC10-
437 PSY b displayed similar structures. The slight differences in fibre concentration and
438 distribution and in the observation of PSY gels are due to variation of sampling. As shown in
439 Figure 2, the majority of FC10 fibres maintained their integrity with smaller fibrils peeled off
440 the main cellulose fibres. This structural similarity is correlated with the similar rheological
441 behaviour that mechanical spectra of heated FC0-PSY and FC10-PSY closely overlapped
442 each other (Figure 6b). As for FC60-PSY, cellulose fibres were processed into smaller FC
443 fibres by a high degree of fibrillation, therefore, they occupied much greater volume and
444 contacted with PSY to a larger degree. The PSY gel, therefore, appeared to be highly filled
445 by F60 fibres with a much denser and clumped structure, which explains the distinct
446 viscoelastic property of FC60-PSY (higher moduli). Similar effects on the strength of

compressed MFC-resin composite were reported by Nakagaito and Yano (2004) that fibrillation treatment on cellulose surfaces is ineffective but fibre disintegration strengthens the composites.

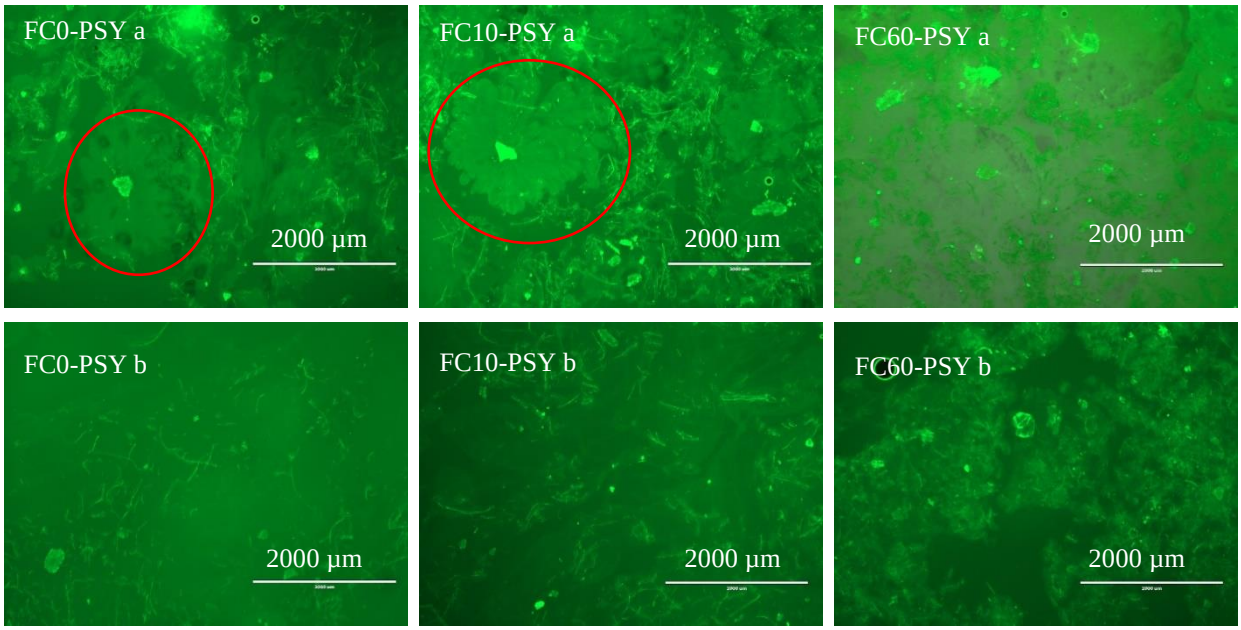

Figure 8. Fluorescent microscopy images of FC and PSY mixtures at a concentration of 0.82% respectively before (a) and after (b) heat treatment. PSY was labelled with FITC shown in green in the images. FC was not specified in colour. The fluorescent image of FC60-PSY was overlapped with the transmitted light microscopy image. A hydrated PSY particle is highlighted in a red circle in FC0-PSY a and FC10-PSY a. Representative images are shown from image acquisitions in at least triplicate.

The concentrations of the mixtures were reduced to 0.25% for each component to further investigate the interactions between FCs and PSY (Figure 9). The three images in the first row present the overall structure of diluted mixtures of FCs and PSY. FC0-PSY and FC10-PSY have similar structures appearing as a dispersion of fibres and particles. Some larger pieces are also observed which might be the epidermis particles of psyllium seeds, cellulose fibre clusters, or PSY polysaccharide aggregates. FC60-PSY is distinct from the other two where lumps with irregular shapes occupied a large volume fraction. The images in the second row present details of FC-PSY mixtures with higher magnifications. According to a previous study (Ren et al., Unpublished results), it is known that PSY is not water-soluble. It existed as gel aggregates, as shown in Figure 9. Some of these aggregates (green) were attached and concentrated to the FC fibres (blue). A similar structure has been observed by Mikkelsen et al. (2015) although, in their study, heteroxylan was incorporated into cellulose

during bacteria fermentation and the scale was much smaller than what is shown in Figure 9. The absorption of heteroxylan aggregates rather than individual molecules to cellulose surface was also observed by Linder, Bergman, Bodin and Gatenholm (2003). In FC60-PSY, cellulose was highly fibrillated and occupied a much larger volume with the larger total surface; therefore, the interaction with PSY was more extensive than FC0 and FC10. FC60 dispersed as fibre clusters, as revealed under transmitted light microscopy (Figure 2) and, when the fibre clusters interacted with PSY gel aggregates, they appeared as lumps (Figure 9).

PSY polysaccharide is composed of a variety of heteroxylans varying in length, composition and distribution of sidechains, which lead to structural differences at the molecular level, different rheological properties and different responses to temperature (Ren et al., Unpublished results). In this study, PSY was also fractionated at different temperatures and the mixtures of PSY fractions and FCs at the concentration of 0.25% are shown in Figure 9. F60 was the most extensively attached to FC0 and FC10 fibres. Other PSY fractions barely associated with FC0 and showed a slight association with FC10 fibres. There was no significant difference between the mixtures of four PSY fractions with FC60. Therefore, it can be concluded that 1) F60 is the main PSY fraction associating with cellulose fibres; 2) the interaction between PSY and cellulose is promoted by fibrillation.

It is usually observed that the association of heteroxylan with cellulose is obstructed by substitution of sidechains or chemical groups (Kabel, van den Borne, Vincken, Voragen & Schols, 2007; Köhnke, Östlund & Brelid, 2011; Mikkelsen et al., 2015). However, as previously reported (Ren et al., Unpublished results), F60 is a highly substituted fraction with a relatively high arabinose content compared to F20 and F40, but only this fraction exhibited a significant association with FC0 (Figure 9). It has been reported that hairy pectin can associate with cellulose via its neutral sugar sidechains including arabinan (Iwai, Ishii & Satoh, 2001; Oechslin, Lutz & Amadò, 2003; Vignon, Heux, Malainine & Mahrouz, 2004). Arabinan adopts a conformation compatible with cellulose binding in terms of surface complementarity, therefore, it aligns with cellulose microfibrils which might be mediated by hydrogen bonds (Zykwinska, Ralet, Garnier & Thibault, 2005). Therefore, it is possible that F60 is branched by relatively long sidechains of arabinan, which associate with cellulose in a similar way as the hairy pectin.

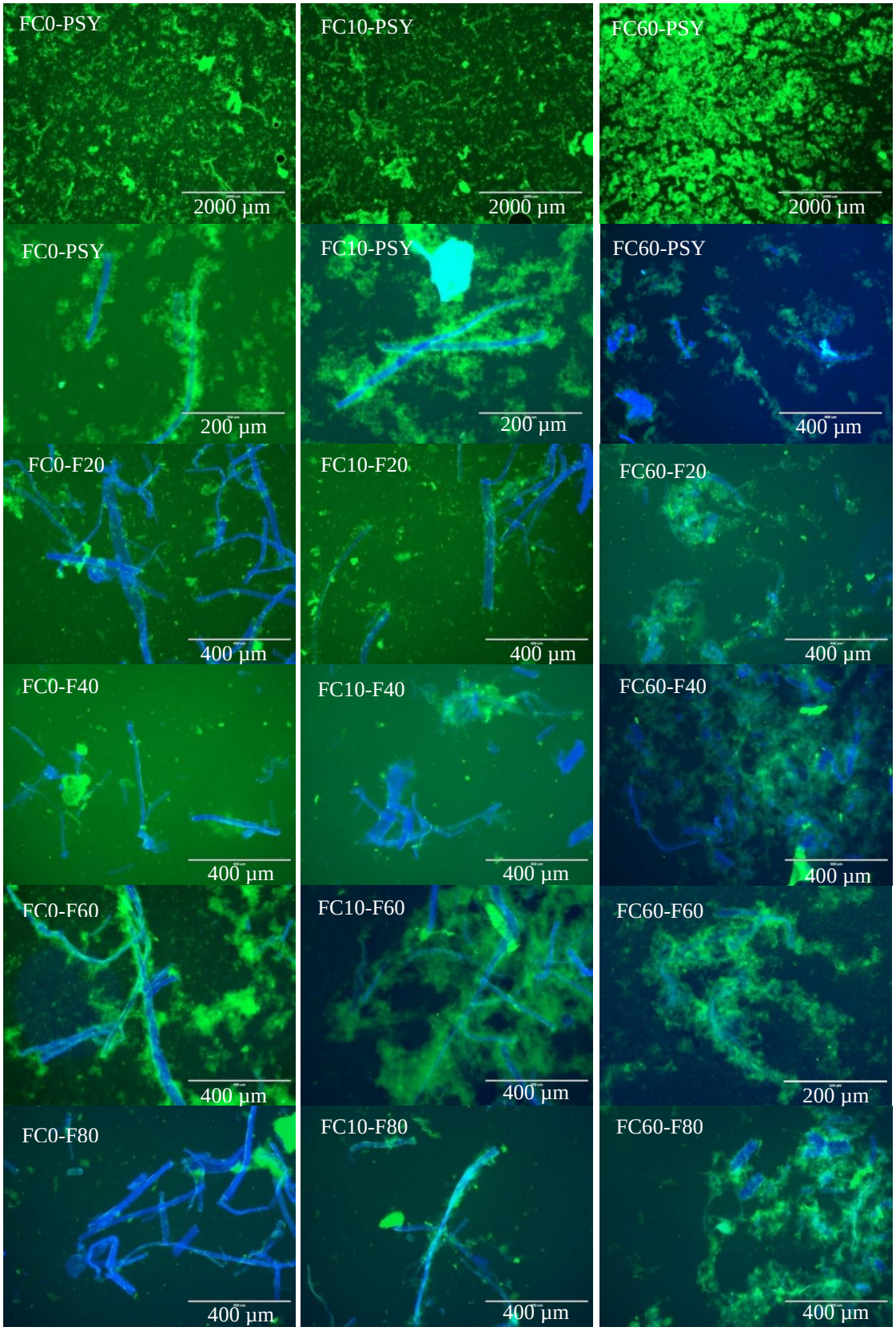

Figure 9. Fluorescent microscopy images of FC and PSY mixtures at a concentration of 0.25% respectively PSY was labelled with FITC shown in green in the images. FC was not specified in

colour in the three images in the first row and it was stained by methyl blue shown in blue in the remaining images. Representative images are shown from image acquisition in at least triplicate.

In addition, the well-known synergistic interactions of xanthan and mannan based polysaccharides provide insights into polysaccharide interactions as a good example. The latest mechanism of the interaction of xanthan with konjac glucomannan has been proposed by Abbaszadeh, MacNaughtan, Sworn and Foster (2016) that two types of interactions are involved at different temperatures, where type A is the interaction with ordered helical xanthan chains while type B is interaction with 2-fold disordered xanthan backbone. A polysaccharide with 2-fold helical conformation is compatible with cellulose allowing interactions between backbones (Busse-Wicher et al., 2016; Preston, 1979). PSY heteroxylans have been hypothesised to contain domains adopting helical conformation, which undergoes softening, helical conformational transition, and melting into coils upon heating, which is similar to xanthan (Ren et al., Unpublished results). According to the similarities to xanthan, Abbaszadeh et al. (2016)'s model could be used and modified to explain the interactions between PSY and cellulose. Some of the helical domains of PSY heteroxylan might be favourable to the association with cellulose. Additionally, a 2 fold helical or coil conformation, if exists as domains on PSY heteroxylan or appears in the conformational transition during heating, could be able to associate, or adapt and associate respectively, with cellulose as a result of stereochemical compatibility (Berry, Davis & Gidley, 2001; Whitney, Brigham, Darke, Reid & Gidley, 1998). However, the softening and melting of PSY heteroxylans is thermal reversible (Ren et al., Unpublished results). In other words, based on the hypothesis, the helical conformation of certain domains of heteroxylan molecules recovers and deviates from coil and 2 fold helical conformation during cooling and become unfavourable to the interaction with cellulose. The higher G' during cooling than G' during heating and the isothermal G' decline shown in Figure 6c and 6d suggest a delay of this molecular conformation recovery and loss of interaction with cellulose which are dependent on both temperature and time.

Another possible mechanism of the association with cellulose relies on the porous structure of cellulose where xyloglucan and heteroxylan can be trapped (Köhnke et al., 2011; Zykwinska et al., 2005). It is reasonable to consider that cellulose with rough surfaces or porous structure provides docking positions where PSY heteroxylan can be immobilised and accumulate. This behaviour was more obvious in FC10 whose surface roughness was

increased by the fibrillation process as shown in the second column of images in Figure 9 that the association between all flour PSY fractions with FC10 increased slightly compared to the association with FC0. However, at a higher concentration, this phenomenon does not significantly affect the structure and the rheological property of the gel composites composed by PSY and FC0 or FC10 (Figure 6b).

FC60 is heavily fibrillated and, as shown in Figure 9, the mixtures of FC60 with both whole PSY and PSY fractions appear to be interpenetrating gels or interpenetrating gel particles. Combining the fact that moduli of heated FC60-PSY were much higher than FC0-PSY and FC10-PSY, the influence of the trapping effect of cellulose on PSY increased and finally overcame the weak interaction between FC and PSY. The interpenetrating structure of FC60-PSY and dense volume occupation dominantly contributed to its overall rheological property. Another approach is considering the contribution to rheological properties of increased volume fractions of FC as reported by Hemar, Lebreton, Xu and Day (2011) that a significant increase of volume fraction leads to the domination of the rheological responses.

4. Conclusion

Fibrillation of cellulose starts from the surface, weak points, and tips of cellulose fibres. It significantly increases the stability and water retention ability of cellulose suspensions. Distance-induced (by centrifugation, leading to reduced distance and increased contacts between fibres) FC flocculates are larger than heat-induced ones. Unheated FC and PSY mixtures can be considered as a binary phase-separated mixture with one phase of hydrated PSY particles and the other one concentrated in FCs. The rheological moduli of unheated mixtures increase with an increase in fibrillation time because fibrillation increases the volume taken by FC fibres. Water competition, originating from thermodynamical incompatibility, between highly fibrillated cellulose and PSY causes greater rheological synergistic behaviour. However, after heat treatment, the mixtures are more similar to interpenetrating gel composites. When the fibrillation only affects the surface of cellulose fibres, there is no significant difference in structure and rheological property. However, the loss of fibres integrity contributes to a distinct denser structure and higher moduli. PSY and its fractions form aggregates, which associate with FC fibres. The heavily substituted PSY heteroxylan (F60) is the only fraction pronouncedly associates with unfibrillated cellulose at room temperature. The association possibly involves interactions between arabinan sidechains of PSY heteroxylan and cellulose surface or/and backbone interactions. The backbone interactions are time and temperature dependent. Additionally, the whole PSY and all fractions can be trapped by cellulose, which becomes more dominant with a high degree

of fibrillation. Summarily, the different temperature fractions of PSY appear to ‘interact’ with FCs both at a molecular level and fibrous interpenetrating but also through incompatibility. In a bulk PSY sample containing mixed molecular structures a complex and multilevel ‘interaction’ takes place and requires more work to fully characterise the structuring approaches. This study provides the possibility of applying the novel mixtures of FC and PSY in designing structured food, pharmaceutical, and cosmetic products.

Acknowledgement

This work was supported by the University of Nottingham (Vice-Chancellor's Scholarship for Research Excellence (International)) and PepsiCo. The views and opinions expressed in this presentation are those of the author and do not necessarily reflect the position or policy of PepsiCo.

Reference

Abbaszadeh, A., MacNaughtan, W., Sworn, G. & Foster, T. J. (2016). New insights into xanthan synergistic interactions with konjac glucomannan: A novel interaction mechanism proposal. *Carbohydrate Polymers, 144*, 168-177.

Agoda-Tandjawa, G., Durand, S., Gaillard, C., Garnier, C. & Doublier, J. L. (2012). Rheological behaviour and microstructure of microfibrillated cellulose suspensions/low-methoxyl pectin mixed systems. Effect of calcium ions. *Carbohydrate Polymers, 87*(2), 1045-1057.

Alemdar, A. & Sain, M. (2008). Isolation and characterization of nanofibers from agricultural residues – Wheat straw and soy hulls. *Bioresource Technology, 99*(6), 1664-1671.

Andresen, M., Johansson, L.-S., Tanem, B. S. & Stenius, P. (2006). Properties and characterization of hydrophobized microfibrillated cellulose. *Cellulose, 13*(6), 665-677.

Andrewartha, K. A., Phillips, D. R. & Stone, B. A. (1979). Solution properties of wheat-flour arabinoxylans and enzymically modified arabinoxylans. *Carbohydrate Research, 77*, 191-204.

Atalla, R. H. & Vanderhart, D. L. (1984). Native cellulose: A composite of two distinct crystalline forms. *Science, 223*(4633), 283-285.

Berry, M. J., Davis, P. J. & Gidley, M. J. (2001). Conjugated polysaccharide fabric detergent and conditioning products. US6225462B1.

Bledzki, A. K. & Gassan, J. (1999). Composites reinforced with cellulose based fibres. *Progress in Polymer Science, 24*(2), 221-274.

Busse-Wicher, M., Grantham, Nicholas J., Lyczakowski, Jan J., Nikolovski, N. & Dupree, P. (2016). Xylan decoration patterns and the plant secondary cell wall molecular architecture. *Biochemical Society Transactions, 44*(1), 74-78.

Carpita, N. C. & Gibeaut, D. M. (1993). Structural models of primary cell walls in flowering plants: consistency of molecular structure with the physical properties of the walls during growth. *The Plant Journal, 3*(1), 1-30.

Chanliaud, E. & Gidley, M. J. (1999). In vitro synthesis and properties of pectin/Acetobacter xylinus cellulose composites. *The Plant Journal, 20*(1), 25-35.

Díaz-Calderón, P., MacNaughtan, B., Hill, S., Foster, T., Enrione, J. & Mitchell, J. (2018). Changes in gelatinisation and pasting properties of various starches (wheat, maize and waxy maize) by the addition of bacterial cellulose fibrils. *Food Hydrocolloids, 80*, 274-280.

Edwards, S., Chaplin, M. F., Blackwood, A. D. & Dettmar, P. W. (2003). Primary structure of arabinoxylans of ispaghula husk and wheat bran. *Proceedings of the Nutrition Society, 62*(1), 217-222.

Farahnaky, A., Askari, H., Majzoobi, M. & Mesbahi, G. (2010). The impact of concentration, temperature and pH on dynamic rheology of psyllium gels. *Journal of Food Engineering, 100*(2), 294-301.

Felby, C., Thygesen, L. G., Kristensen, J. B., Jorgensen, H. & Elder, T. (2008). Cellulose-water interactions during enzymatic hydrolysis as studied by time domain NMR. *Cellulose, 15*(5), 703-710.

Fischer, M. H., Yu, N. X., Gray, G. R., Ralph, J., Anderson, L. & Marlett, J. A. (2004). The gel-forming polysaccharide of psyllium husk (Plantago ovata Forsk). *Carbohydrate Research, 339*(11), 2009-2017.

Foster, T., Russell, A., Farrer, D., Golding, M., Finlayson, R., Thomas, A., Jarvis, D. & Pelan, E. (2007). Instant emulsions. In E. Dickinson & M. E. Leser (Eds.), *Food Colloids: Self-Assembly and Material Science* (pp. 413-422). Cambridge Royal Society of Chemistry.

Goldberg, R. N., Schliesser, J., Mittal, A., Decker, S. R., Santos, A. F. L. O. M., Freitas, V. L. S., Urbas, A., Lang, B. E., Heiss, C., Ribeiro da Silva, M. D. M. C., Woodfield, B. F., Katahira, R., Wang, W. & Johnson, D. K. (2015). A thermodynamic investigation of the cellulose allomorphs: Cellulose(am), cellulose Iβ(cr), cellulose II(cr), and cellulose III(cr). *The Journal of Chemical Thermodynamics, 81*, 184-226.

Grantham, N. J., Wurman-Rodrich, J., Terrett, O. M., Lyczakowski, J. J., Stott, K., Iuga, D., Simmons, T. J., Durand-Tardif, M., Brown, S. P., Dupree, R., Busse-Wicher, M. & Dupree, P. (2017). An even pattern of xylan substitution is critical for interaction with cellulose in plant cell walls. *Nature Plants, 3*(11), 859-865.

Guo, Q., Cui, S. W., Wang, Q., Goff, H. D. & Smith, A. (2009). Microstructure and rheological properties of psyllium polysaccharide gel. *Food Hydrocolloids, 23*(6), 1542-1547.

Guo, Q., Cui, S. W., Wangb, Q. & Young, J. C. (2008). Fractionation and physicochemical characterization of psyllium gum. *Carbohydrate Polymers, 73*(1), 35-43.

Habibi, Y., Lucia, L. A. & Rojas, O. J. (2010). Cellulose nanocrystals: Chemistry, self-assembly, and applications. *Chemical Reviews, 110*(6), 3479-3500.

Haque, A., Richardson, R. K., Morris, E. R. & Dea, I. C. M. (1993). Xanthan-like weak gel rheology from dispersions of ispaghula seed husk. *Carbohydrate Polymers, 22*(4), 223-232.

Hebert, J. J. (1985). Crystalline form of native celluloses. *Science, 227*(4682), 79-79.

Heiskanen, I., Harlin, A., Backfolk, K. & Laitinen, R. (2014). Process for the production of microfibrillated cellulose in an extruder and microfibrillated cellulose produced according to the process. In: Google Patents.

Hemar, Y., Lebreton, S., Xu, M. & Day, L. (2011). Small-deformation rheology investigation of rehydrated cell wall particles–xanthan mixtures. *Food Hydrocolloids, 25*(4), 668-676.

Herrick, F. W., Casebier, R. L., Hamilton, J. K. & Sandberg, K. R. (1983). Microfibrillated cellulose: morphology and accessibility. In *Journal of Applied Polymer Science: Applied Polymer Symposium;(United States)* (Vol. 37): ITT Rayonier Inc., Shelton, WA.

Huber, G. W., Iborra, S. & Corma, A. (2006). Synthesis of transportation fuels from biomass: chemistry, catalysts, and engineering. *Chemical Reviews, 106*(9), 4044-4098.

Ibbett, R., Wortmann, F., Varga, K. & Schuster, K. C. (2014). A morphological interpretation of water chemical exchange and mobility in cellulose materials derived from proton NMR T-2 relaxation. *Cellulose, 21*(1), 139-152.

Iwai, H., Ishii, T. & Satoh, S. (2001). Absence of arabinan in the side chains of the pectic polysaccharides strongly associated with cell walls of Nicotiana plumbaginifolia non-organogenic callus with loosely attached constituent cells. *Planta, 213*(6), 907-915.

Iwamoto, S., Nakagaito, A. N., Yano, H. & Nogi, M. (2005). Optically transparent composites reinforced with plant fiber-based nanofibers. *Applied Physics A, 81*(6), 1109-1112.

Izydorczyk, M. S., Macri, L. J. & MacGregor, A. W. (1998). Structure and physicochemical properties of barley non-starch polysaccharides—II. Alkaliextractable β-glucans and arabinoxylans. *Carbohydrate Polymers, 35*(3), 259-269.

Kabel, M. A., van den Borne, H., Vincken, J.-P., Voragen, A. G. J. & Schols, H. A. (2007). Structural differences of xylans affect their interaction with cellulose. *Carbohydrate Polymers, 69*(1), 94-105.

Kale, M. S., Yadav, M. P. & Hanah, K. A. (2016). Suppression of Psyllium Husk Suspension Viscosity by Addition of Water Soluble Polysaccharides. *Journal of Food Science, 81*(10), E2476-E2483.

Köhnke, T., Östlund, Å. & Brelid, H. (2011). Adsorption of arabinoxylan on cellulosic surfaces: Influence of degree of substitution and substitution pattern on adsorption characteristics. *Biomacromolecules, 12*(7), 2633-2641.

Lavoine, N., Desloges, I., Dufresne, A. & Bras, J. (2012). Microfibrillated cellulose – Its barrier properties and applications in cellulosic materials: A review. *Carbohydrate Polymers, 90*(2), 735-764.

Li, D. & Xia, Y. (2004). Electrospinning of nanofibers: Reinventing the wheel? *Advanced Materials, 16*(14), 1151-1170.

Linder, Å., Bergman, R., Bodin, A. & Gatenholm, P. (2003). Mechanism of assembly of xylan onto cellulose surfaces. *Langmuir, 19*(12), 5072-5077.

López-Rubio, A., Lagaron, J. M., Ankerfors, M., Lindström, T., Nordqvist, D., Mattozzi, A. & Hedenqvist, M. S. (2007). Enhanced film forming and film properties of amylopectin using micro-fibrillated cellulose. *Carbohydrate Polymers, 68*(4), 718-727.

Mandalari, G., Faulds, C. B., Sancho, A. I., Saija, A., Bisignano, G., LoCurto, R. & Waldron, K. W. (2005). Fractionation and characterisation of arabinoxylans from brewers' spent grain and wheat bran. *Journal of Cereal Science, 42*(2), 205-212.

Meiboom, S. & Gill, D. (1958). Modified Spin‐Echo method for measuring nuclear relaxation times. *Review of Scientific Instruments, 29*(8), 688-691.

Mengual, O., Meunier, G., Cayré, I., Puech, K. & Snabre, P. (1999). TURBISCAN MA 2000: multiple light scattering measurement for concentrated emulsion and suspension instability analysis. *Talanta, 50*(2), 445-456.

Mikkelsen, D., Flanagan, B. M., Wilson, S. M., Bacic, A. & Gidley, M. J. (2015). Interactions of arabinoxylan and (1,3)(1,4)-β-glucan with cellulose networks. *Biomacromolecules, 16*(4), 1232-1239.

Mohanty, A. K., Misra, M. & Hinrichsen, G. (2000). Biofibres, biodegradable polymers and biocomposites: An overview. *Macromolecular Materials and Engineering, 276-277*(1), 1-24.

Nakagaito, A. N. & Yano, H. (2004). The effect of morphological changes from pulp fiber towards nano-scale fibrillated cellulose on the mechanical properties of high-strength plant fiber based composites. *Applied Physics a-Materials Science & Processing, 78*(4), 547-552.

Nishiyama, Y., Sugiyama, J., Chanzy, H. & Langan, P. (2003). Crystal structure and hydrogen bonding system in cellulose Iα from synchrotron X-ray and neutron fiber diffraction. *Journal of the American Chemical Society, 125*(47), 14300-14306.

Oechslin, R., Lutz, M. V. & Amadò, R. (2003). Pectic substances isolated from apple cellulosic residue: structural characterisation of a new type of rhamnogalacturonan I. *Carbohydrate Polymers, 51*(3), 301-310.

Pääkkö, M., Ankerfors, M., Kosonen, H., Nykänen, A., Ahola, S., Österberg, M., Ruokolainen, J., Laine, J., Larsson, P. T., Ikkala, O. & Lindström, T. (2007). Enzymatic hydrolysis combined with mechanical shearing and high-pressure homogenization for nanoscale cellulose fibrils and strong gels. *Biomacromolecules, 8*(6), 1934-1941.

Preston, R. D. (1979). Polysaccharide conformation and cell wall function. *Annual Review of Plant Physiology, 30*(1), 55-78.

Quiévy, N., Jacquet, N., Sclavons, M., Deroanne, C., Paquot, M. & Devaux, J. (2010). Influence of homogenization and drying on the thermal stability of microfibrillated cellulose. *Polymer Degradation and Stability, 95*(3), 306-314.

Rao, M. R. P., Warrier, D. U., Gaikwad, S. R. & Shevate, P. M. (2016). Phosphorylation of psyllium seed polysaccharide and its characterization. *International Journal of Biological Macromolecules, 85*, 317-326.

Ren, Y., Yakubov, G., Linter, B. R., MacNaughtan, B. & Foster, T. J. (Unpublished results). Temperature fractionation, and physicochemical and rheological analysis of psyllium. *Manuscript submitted for publication*.

Siró, I. & Plackett, D. (2010). Microfibrillated cellulose and new nanocomposite materials: a review. *Cellulose, 17*(3), 459-494.

Stenstad, P., Andresen, M., Tanem, B. S. & Stenius, P. (2008). Chemical surface modifications of microfibrillated cellulose. *Cellulose, 15*(1), 35-45.

Sugiyama, J., Persson, J. & Chanzy, H. (1991). Combined infrared and electron diffraction study of the polymorphism of native celluloses. *Macromolecules, 24*(9), 2461-2466.

Sullo, A. (2012). *Self-association of cellulose ethers and its effect on the starch gelatinisation.* University of Nottingham, Nottingham.

Svagan, A. J., Azizi Samir, M. A. S. & Berglund, L. A. (2007). Biomimetic polysaccharide nanocomposites of high cellulose content and high toughness. *Biomacromolecules, 8*(8), 2556-2563.

Turbak, A. F., Snyder, F. W. & Sandberg, K. R. (1982). Food products containing microfibrillated cellulose. US4341807.

Turbak, A. F., Snyder, F. W. & Sandberg, K. R. (1983a). Microfibrillated cellulose. US4374702A.

Turbak, A. F., Snyder, F. W. & Sandberg, K. R. (1983b). Suspensions containing microfibrillated cellulose. US4378381A.

Vignon, M. R., Heux, L., Malainine, M. E. & Mahrouz, M. (2004). Arabinan–cellulose composite in Opuntia ficus-indica prickly pear spines. *Carbohydrate Research, 339*(1), 123-131.

Wada, M., Chanzy, H., Nishiyama, Y. & Langan, P. (2004). Cellulose IIII crystal structure and hydrogen bonding by synchrotron X-ray and neutron fiber diffraction. *Macromolecules, 37*(23), 8548-8555.

Walther, A., Timonen, J. V. I., Díez, I., Laukkanen, A. & Ikkala, O. (2011). Multifunctional high-performance biofibers based on wet-extrusion of renewable native cellulose nanofibrils. *Advanced Materials, 23*(26), 2924-2928.

Wang, B. & Sain, M. (2007). Dispersion of soybean stock-based nanofiber in a plastic matrix. *Polymer International, 56*(4), 538-546.

Whitney, S. E., Gothard, M. G., Mitchell, J. T. & Gidley, M. J. (1999). Roles of cellulose and xyloglucan in determining the mechanical properties of primary plant cell walls. *Plant Physiology, 121*(2), 657-664.

Whitney, S. E. C., Brigham, J. E., Darke, A. H., Reid, J. S. G. & Gidley, M. J. (1998). Structural aspects of the interaction of mannan-based polysaccharides with bacterial cellulose. *Carbohydrate Research, 307*(3), 299-309.

Whitney, S. E. C., Wilson, E., Webster, J., Bacic, A., Reid, J. S. G. & Gidley, M. J. (2006). Effects of structural variation in xyloglucan polymers on interactions with bacterial cellulose. *American Journal of Botany, 93*(10), 1402-1414.

Wyman, C. E., Decker, S. R., Himmel, M. E., Brady, J. W., Skopec, C. E. & Viikari, L. (2005). hydrolysis of cellulose and hemicellulose. In S. Dumitriu (Ed.), *Polysaccharides: Structural Diversity and Functional Versatility* (2nd ed., pp. 995 - 1034). New York: Marcel Dekker.

Yu, L., DeVay, G. E., Lai, G. H., Simmons, C. T. & Neilsen, S. R. (2001). Enzymatic modification of psyllium. US6248373B1.

Yu, L., Yakubov, G. E., Zeng, W., Xing, X., Stenson, J., Bulone, V. & Stokes, J. R. (2017). Multi-layer mucilage of Plantago ovata seeds: Rheological differences arise from variations in arabinoxylan side chains. *Carbohydrate Polymers, 165*, 132-141.

Zhang, Z. X., Smith, C. & Li, W. L. (2014). Extraction and modification technology of arabinoxylans from cereal by-products: A critical review. *Food Research International, 65*, 423-436.

Zimmermann, T., Pöhler, E. & Geiger, T. (2004). Cellulose fibrils for polymer reinforcement. *Advanced Engineering Materials, 6*(9), 754-761.

Zykwinska, A. W., Ralet, M.-C. J., Garnier, C. D. & Thibault, J.-F. J. (2005). Evidence for in vitro binding of pectin side chains to cellulose. *Plant Physiology, 139*(1), 397-407.